MOLECULAR IMAGING AND BIOLOGY

Mol Imaging Biol (2019) 21:375–381
DOI: 10.1007/s11307-018-1247-2

Published Online: 9 July 2018

RESEARCH ARTICLE

Linked Hexokinase and Glucose-6-Phosphatase Activities Reflect Grade of Ovarian Malignancy

Birgitte Brinkmann Olsen,[1,2] Albert Gjedde,[1,2] Mie Holm Vilstrup,[1] Iben Birgit Gade Johnsen,[3] Gudrun Neumann,[4] Drew Avedis Torigian,[5] Abass Alavi,[5] Poul Flemming Høilund-Carlsen[1,2]

[1]*Department of Nuclear Medicine, Odense University Hospital, Kløvervænget 47, 5000, Odense, Denmark*
[2]*Department of Clinical Research, University of Southern Denmark, Odense, Denmark*
[3]*Department of Clinical Pathology, Odense University Hospital, Odense, Denmark*
[4]*Department of Gynecology and Obstetrics, Odense University Hospital, Odense, Denmark*
[5]*Department of Radiology, University of Pennsylvania School of Medicine, Hospital of the University of Pennsylvania, Philadelphia, USA*

Abstract

Purpose: Malignant cells exhibit increased rates of aerobic glycolysis. Here, we tested whether the accumulation of fluoro-deoxyglucose-6-phosphate (FDG6P) in ovarian cancers of differential malignancy reflects inversely correlated elevations of hexokinase (HK) and glucose-6-phosphatase (G6Pase) activities.

Procedures: Twenty-nine women with suspected ovarian cancer had positron emission tomography (PET) prior to surgery. From fresh-frozen tissue, we determined the activities of HK and G6Pase, and from the PET images, we determined the tumor maximum standardized uptake value (SUVmax) of 2-deoxy-2-[^{18}F]fluoro-D-glucose.

Results: The SUVmax of malignant lesions significantly exceeded the SUVmax of benign ($p < 0.005$) and borderline lesions ($p < 0.0005$) that did not differ significantly. We found no significant correlation between measured HK or G6Pase activities and histological tumor type or SUVmax except that G6Pase activities were higher in malignant than borderline lesions ($p < 0.05$). Measured HK and G6Pase activities correlated inversely ($p < 0.05$). The slopes from the regression lines of the three correlations yielded positively correlated abscissa and ordinate intercepts, designated HK_{max} and $G6Pase_{max}$, respectively ($r = 0.67$, $p < 0.0001$). The positive correlations between the abscissa and ordinate intercepts with SUVmax had regression coefficients of $r = 0.44$, $p < 0.05$; and $r = 0.39$, $p < 0.05$, respectively.

Conclusions: The results distinguished two ovarian cancer phenotypes, one with elevated HK activity and low G6Pase activity, and another with the opposite characteristics.

Key Words: Ovarian cancer, FDG, Glucose-6-phosphatase, Hexokinase, Positron emission tomography (PET)

Introduction

Ovarian cancer is the leading cause of death from gynecological malignancies [1], but the symptoms and signs are often vague. When finally diagnosed, the malignancy can be advanced. The combination of positron emission tomography (PET) with 2-

Electronic supplementary material The online version of this article (https://doi.org/10.1007/s11307-018-1247-2) contains supplementary material, which is available to authorized users.

Correspondence to: Birgitte Olsen; *e-mail:* birgitte.brinkmann.olsen@rsyd.dk

deoxy-2-[^{18}F]fluoro-D-glucose ([^{18}F]FDG) and X-ray computed tomography (CT) is important to cancer staging, therapy monitoring, and prediction of clinical outcome in patients with malignant tumors, including ovarian cancer [2–4]. The molecular imaging exploits the increased rate of aerobic glycolysis by malignant cells (Warburg Effect) [5]. [^{18}F]FDG is transported into cells by means of facilitated diffusion mediated by the glucose transporters, a large family of proteins of which the insulin-independent glucose transporter 1 (GLUT1) often is overexpressed in cancer cells [6]. Once inside the cells, the glucose analogue [^{18}F]FDG is readily phosphorylated by hexokinases, of which hexokinase 2 (HK2) is highly expressed in cancer cells [7]. Unlike glucose-6-phosphate (G6P), the metabolite FDG-6-phosphate (FDG6P) is not further metabolized and therefore is trapped since it is not subject to dephosphorylation by glucose-6-phosphatase (G6Pase). The increase of FDG6P accumulation in malignant cells is associated with relative magnitudes of uptake, phosphorylation, and dephosphorylation, depending on the relative activities of GLUT1, HK2, and G6Pase, respectively. Several attempts have been made to correlate the expression of these proteins, especially GLUT1 and to a lesser extent HK2, with the trapping of [^{18}F]FDG metabolites in gynecological malignancies. However, the results are unclear and little is known about the contributions of G6Pase [8–16]. In ovarian cancer, only one study addressed the mechanism of [^{18}F]FDG metabolite accumulation, revealing a significant correlation between the expression of GLUT1 and the uptake of FDG in 17 patients with epithelial ovarian cancer [8], but HK and G6Pase activities were not assayed. The concentrations of glucose and G6P are linked in a circle of reactions mediated by the respective enzymes HK and G6Pase that include (1) HK bound to mitochondria and regulated by G6P in the cytosol, and (2) the G6Pase in the endoplasmic reticulum (ER) that reconverts G6P to glucose [17, 18]. The linkage is provided by the activity of the G6P-affine glucose-6-phosphate translocase (G6PT) in the ER membrane that connects the HK and G6Pase steps of the circle [19].

Here, we tested the hypothesis that activities of HK and G6Pase maintain an inverse correlation, as reflected in the cellular concentrations of glucose and glucose-6-phosphate. We correlated the findings with [^{18}F]FDG uptake and tumor histology in order to uncover the mechanism responsible for variable [^{18}F]FDG metabolite accumulations in ovarian cancer.

Patients and Methods

Patients

We included 29 women (aged 40–87 years) suspected of having ovarian cancer. Inclusion criteria were a pre-operative PET/CT scan and availability of freshly frozen tumor tissue. The study was approved by the Regional Ethics Committee of the Region of Southern Denmark and conducted in compliance with Good Clinical Practice, the Declaration of Helsinki, and other applicable regulatory requirements. Six patients were enrolled retrospectively, with previously obtained formal consent to retroactive use of tissue still valid, while 23 patients were enrolled prospectively after both oral and written information and signed consent.

Image Acquisition and Analysis

After at least 6 h of fasting, patients underwent PET/CT imaging 1 h after the intravenous injection of 4 MBq/kg [^{18}F]FDG. Imaging used PET/CT scanners (General Electric, Milwaukee, WI, USA) according to guidelines [20]. A helical diagnostic CT scan (120 kV, Smart mA—max 400 mA, noise index 25, iterative reconstruction ASIR 50 %) was performed followed by a PET scan using a whole-body acquisition protocol. Acquisition time was 2.5 min/bed position, and the scan field of view was 70 cm. The low-dose CT scan was used for attenuation correction. PET images were reconstructed using iterative algorithms (OSEM, 2 iterations/28 subsets) into transaxial slices (standard field of view 50 cm) with a slice thickness of 3.75 mm. A nuclear medicine physician analyzed images with a GE Advantage workstation 4.4. In each patient, SUVmax of the primary ovarian tumor was calculated, which is a semi-quantitative measurement for [^{18}F]FDG uptake in the tumor corrected for injected amount of radiotracer and the distribution volume (patient weight), as follows:

$$\text{SUVmax} = \text{Tumor activity (MBq/g)}/[\text{Injected dose (MBq)}/\text{weight (g)}].$$

Enzyme Activity Assays

Freshly frozen tumor tissue, taken from the visually most malignant area, was crushed in liquid nitrogen using a pestle and mortar. The powdered tissue was lysed in lysis buffer (50 mM Tris-HCl pH 8.0, 1 mM DTT, 150 mM NaCl, 10 % glycerol, 1 % digitonin, protease inhibitor cocktail (Roche)) for 20 min on ice. The lysate was separated by centrifugation 10 min, 10,000×*g* at 4 °C and the pellet discarded. The protein concentration in the supernatant was determined according to the method of Bradford [21]. Fifty micrograms of lysate was used to measure the activity of HK using a colorimetric kinetic hexokinase assay. Briefly, 50 µg of lysate was incubated for 30 min at room temperature in a final volume of 100 µl in assay buffer (50 mM Tris-HCl pH 8.0, 13.3 mM $MgCl_2$, 200 mM glucose, 0.8 mM ATP, 0.8 mM NADPH, 1 U/ml glucose-6-phosphate dehydrogenase and 0.5 mM 2-(4-indophenyl)-3-(4-nitrophenyl)-5-(2,4-disulfophenyl-2H tetrazolium). The color development was measured at 450 nm and the activity of HK was calculated based on a standard curve of NADPH and calculated as µmol NADPH min^{-1} mg^{-1} protein. To determine G6Pase activity, 50 µg of protein extract was incubated with assay buffer (100 mM Bis-Tris pH 6.5, 40 mM glucose) in 650 µl final volume for 10 min at 37 °C. The reaction was stopped by adding 150 µl 30 % trichloroacetic acid. After centrifugation (10 min, 1800×*g*), the supernatant was used for

determination of liberated inorganic phosphate according to [22]. Briefly, 150 µl of supernatant was mixed with 150 µl Taussky-Shorr color reagent (1 % ammonium molybdate, 0.5 M sulfuric acid, 5 % ferrous sulfate) and incubated for 10 min at room temperature. The absorbance at 660 nm was measured and µmol liberated phosphorous was determined based on a phosphorous standard solution. The activity was expressed in µmol phosphorus min^{-1} mg^{-1} protein.

Graphical and Statistical Analysis

Values given in the "Results" section are ranges followed by means ± standard deviations in parentheses. From the inverse correlations of measured activities of HK and G6Pase, we calculated the HK_{max} and $G6Pase_{max}$ intercepts from the linear regressions (Table S1, see electronic supplementary material (ESM))

$$HK_{max} = A_{HK} - \alpha A_{G6Pase}$$

where A represents the measured activities of the two enzymes, and α is the slope of the linear regression, and

$$G6Pase_{max} = A_{G6Pase} - \alpha A_{HK}$$

where correlations between the variables were evaluated by Pearson's correlation coefficient (r). All statistical analyses were performed using Prism 6 (GraphPad Software, Inc., La Jolla, CA), with probabilities (p) less than 0.05 considered statistically significant.

Results

Based on the tumor histology from the 29 patients, 5 had benign tumors, 4 had borderline tumors, and the remaining 20 had malignant tumors. The majority of the malignant tumors were serous adenocarcinomas (17/20), with additional subtypes including mucinous, endometrioid, and clear cell adenocarcinomas. The tumor histologies are summarized in Table 1 and the population characteristics are included in Table S2 (ESM). The SUVmax of the lesions ranged from 1.9 to 48.3 (14.5 ± 11.4) and was significantly higher for the malignant lesions than for the benign ($p < 0.005$) or borderline lesions ($p < 0.0005$) (Fig. 1a), although we found no significant difference of SUVmax between benign and borderline lesions. The enzymatic activities of HK ranged from 1.57 to 21.8 µmol min^{-1} mg^{-1} (10.5 ± 4.8), but we found no significant correlation between HK activity and tumor histology, although there was higher HK activity in borderline and malignant lesions than in benign lesions (Fig. 1b). The measured activities of G6Pase ranged from 0.06 to 0.59 µmol min^{-1} mg^{-1} (0.29 ± 0.14), and we found significantly higher G6Pase enzymatic activity in malignant lesions than in borderline lesions ($p < 0.05$) but no significant difference between malignant and benign lesions, although the activity was higher in the malignant lesions (Fig. 1c).

Table 1.. Histological assessment of ovarian tumors

Histological assessment	No. patients
Malignant tumors	20
Serous adenocarcinoma	17
Grade 1	1
Grade 2	8
Grade 3	8
Mucinous adenocarcinoma	1
Endometrioid adenocarcinoma	1
Grade 1	1
Clear cell adenocarcinoma	1
Borderline	4
Mucinous cystadenoma	2
Serous cystadenoma	2
Benign	5
Fibroma	1
Adenofibroma	1
Mucinous cystadenoma	1
Serous cystadenoma	1
Endometriosis	1

There were significant negative correlations between the measured enzymatic activities of HK (A_{HK}) and G6Pase (A_{G6Pase}) for all three subject groups, as shown in Fig. 2a and Table 2.

Next, we used the slopes of the linear regressions in Fig. 2a (given by $y = \alpha x + b$, where α is the slope of the regression and b is the intercept with the y-axis to calculate the intercepts (referred to here as maximal enzymatic activities HK_{max} and $G6Pase_{max}$) for all subjects individually (Table S1 (ESM))).The correlation of these calculated maximal enzymatic activities was highly significant (Fig. 2b), in agreement with the inverse correlation between the measured activities for the three groups.

Correlations between [^{18}F]FDG uptake and the measured activities of HK and G6Pase are summarized in Table 3. The measured activities of HK and G6Pase did not correlate significantly with SUVmax, irrespective of whether all patients, borderline and malignant, or only malignant cases, were included (Fig. 3a, b). However, both calculated maximum activities correlated significantly with the values of SUVmax (Fig. 3c, d).

Discussion

In order to fully interpret clinical PET findings of tumor metabolism with [^{18}F]FDG, the mechanisms that regulate [^{18}F]FDG phosphorylation and dephosphorylation must be understood. Here, we measured the activities of HK and G6Pase in freshly frozen tissue samples from 29 women with ovarian cancers and correlated the findings with estimates of [^{18}F]FDG uptake and diagnosis. We found that SUVmax was significantly higher in the malignant lesions compared to borderline and benign lesions, as previously described [23–25]. The accumulation of the prevailing [^{18}F]FDG metabolite in the form of FDG6P was reflected in the measure of SUVmax. However, the details of the interactions of tumor HK and G6Pase activities that explain

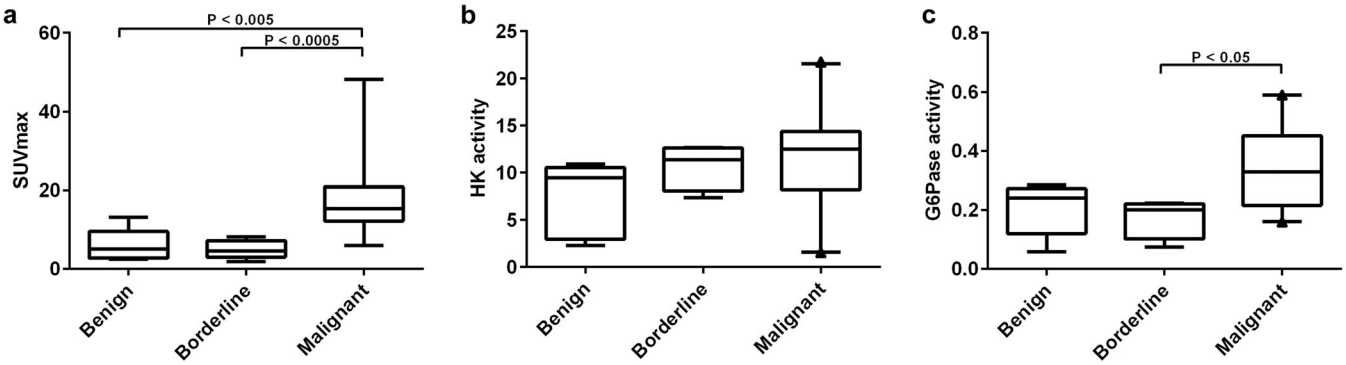

Fig. 1 Box plots illustrating the SUVmax, HK activity, and G6Pase activity for the benign, borderline, and malignant lesions. **a** SUVmax was significantly higher in the malignant lesions compared to borderline and benign lesions. **b** HK activity was not significantly different between lesion groups. **c** G6Pase activity was significantly higher in the malignant lesions compared the borderline lesions. The boxes represent the range between the 25th and 75th percentiles with a horizontal line at the median. The bars delineate the 5th and 95th percentiles.

the increased accumulation of FDG6P in malignant tissues are not known. We found that the measured HK and G6Pase enzymatic activities had significant inverse correlation. SUVmax did not correlate with separate measured HK or G6Pase activities but with the calculated maximum activities, suggesting that neither enzyme activity alone regulates the accumulation of [^{18}F]FDG metabolites in ovarian cancer. Rather, both enzymes are involved in regulating the accumulation, and the [^{18}F]FDG-derived signal reflects accumulated FDG6P in the cytosol when the HK activity is high and accumulated [^{18}F]FDG in the ER when the G6Pase activity is high (Fig. 4).

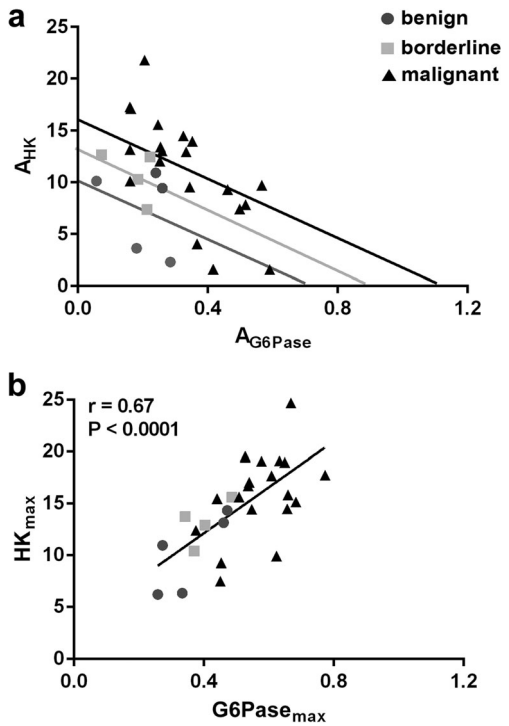

Fig. 2 Correlation between the measured enzymatic activities of HK and G6Pase. **a** The enzymatic activity of HK (A_{HK}) was inversely correlated with the enzymatic activity of G6Pase (A_{G6Pase}). **b** The calculated maximal enzymatic activity of hexokinase (HK_{max}) was significantly correlated with that of G6Pase ($G6Pase_{max}$).

The high activity of HK in malignant tumors and borderline changes compared to benign tumors agrees with results from Jin et al. who reported increased HK2 expression in epithelial ovarian tumors [26]. However, increased HK activity in malignancy also reflects increased binding of HK to the mitochondrial voltage-dependent anion channel, which controls the availability of mitochondrially generated ATP, protects against proteolytic degradation, and abolishes product inhibition by G6P [27], and furthermore, HK is activated by glucagon-like peptide-1 [28, 29]. We also found numerically higher enzymatic activity of G6Pase in the malignant tumors, significantly different from borderline tumors, although not significantly different from benign tumors. Recently, G6Pase was found to be upregulated in glioblastoma multiforme compared to normal brain tissue [30], and to be overexpressed in ovarian cancers in correlation with shorter overall survival [31]. Both in ovarian cancer and glioblastoma multiforme, elimination of G6Pase inhibited the aggressive phenotype [30, 31], suggesting a pro-tumorigenic role for G6Pase.

The present results are also in agreement with a role of G6Pase in invasion, as the non-invasive borderline tumors had

Table 2.. Correlations between measured enzymatic activities

	HK	
	r	*p*
All tumors ($n = 29$)		
G6Pase	− 0.45	0.015
Borderline + malignant ($n = 24$)		
G6Pase	− 0.62	0.002
Malignant ($n = 20$)		
G6Pase	− 0.71	0.0005

Table 3.. Correlations between SUVmax and measured enzymatic activities

	SUVmax	
	r	*p*
All tumors ($n = 29$)		
HK	0.36	0.06
G6Pase	0.1	0.61
Borderline + malignant ($n = 24$)		
HK	0.29	0.17
G6Pase	− 0.01	0.96
Malignant ($n = 20$)		
HK	0.25	0.28
G6Pase	− 0.08	0.72

lower G6Pase activity compared to the malignant tumors [32]. Interestingly, the present results also indicate that it might be possible to distinguish borderline from benign and malignant tumors by measuring HK and G6Pase activity, respectively, but with a need for testing the relationship between HK and G6Pase activity and stages in ovarian cancer in a larger setting.

We have shown the existence of two different ovarian cancer phenotypes, based on glucose metabolism. One is a glycolytic phenotype with a high rate of glycolysis (high HK activity) and a concomitant low rate of gluconeogenesis (low G6Pase activity). The other phenotype is characterized by a higher rate of gluconeogenesis (high G6Pase activity) and a concomitantly lower rate of glycolysis (low HK activity). These results suggest that one patient group could benefit from treatment with a HK inhibitor, whereas the other group could benefit from G6Pase inhibition. Elimination of HK or G6Pase has previously been shown to be effective in inhibiting cancer cell growth and decreasing tumor burden in animals [31, 33]. Hence, the present results suggest that profiling whether a tumor is "glycolytic" or "gluconeogenetic" would have a large impact on future treatment in the context of personalized medicine.

A weakness of this study is the relatively small number of patients. Furthermore, tumor heterogeneity should be considered with respect to correlations between [^{18}F]FDG uptake and enzymatic activity. In practice, it is almost impossible to precisely identify the most [^{18}F]FDG-avid parts of a tumor seen with PET with the excised material used for further analysis. Future experiments in pre-clinical animal models may shed light on the cellular and molecular mechanisms responsible for [^{18}F]FDG uptake in ovarian cancers. Finally, measuring the levels also of GLUT1 would have yielded information about all three processes (uptake, phosphorylation, and dephosphorylation), although this was not possible with the available material. The strengths of the

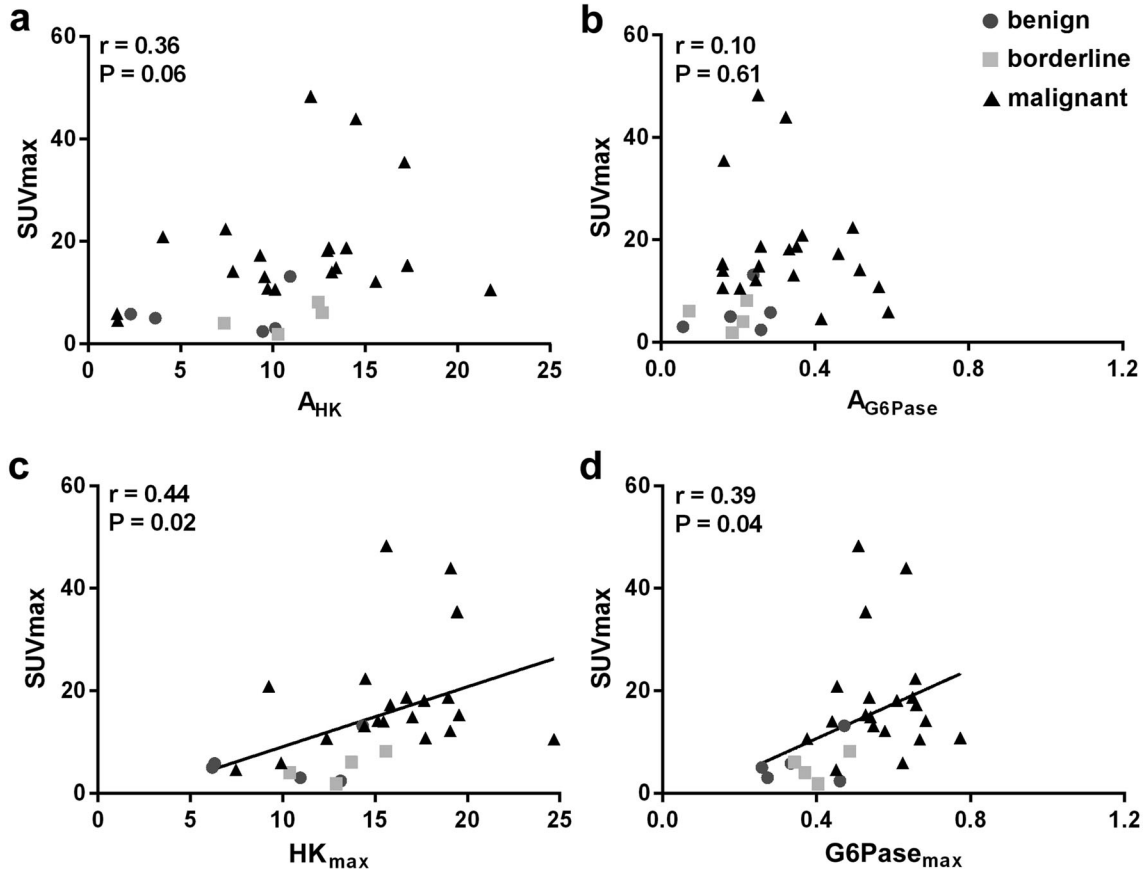

Fig. 3 Correlations between [^{18}F]FDG uptake and the enzymatic activities of HK and G6Pase. **a** The measured enzymatic activity of HK and **b** the measured enzymatic activity of G6Pase did not correlate with SUVmax. However, the calculated maximal enzymatic activities **c** HK and **d** G6Pase were both correlated with SUVmax.

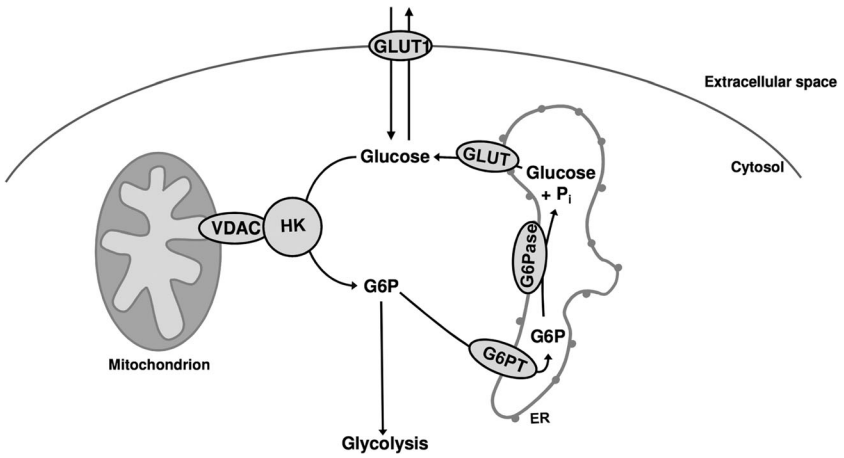

Fig. 4 Model for the link between HK and G6Pase. [^{18}F]FDG enters the cell *via* glucose transporters located at the plasma membrane. Once inside cells, [^{18}F]FDG is phosphorylated by HK, bound to VDAC at the mitochondrial membrane. The resulting FDG6P cannot enter the glycolytic pathway and is transported into the ER lumen through G6PT located in the ER membrane. Inside the ER, FDG6P is dephosphorylated by G6Pase and the resulting FDG6P exits the ER through glucose transporters and eventually the cell. Thus, accumulation of [^{18}F]FDG seen on PET scans can be due to high [^{18}F]FDG in the cytosol or high FDG6P in the ER. VDAC voltage-dependent anion channel, HK hexokinase, G6Pase glucose-6-phosphatase, glut glucose transporter, Pi inorganic phosphate, G6PT glucose-6-phosphate transporter, ER endoplasmic reticulum.

study are the measurements of the activity of the enzymes rather than the expression level (protein or mRNA), and the analysis of a spectrum of ovarian cancers ranging from benign to borderline to malignant.

Conclusions

We found no significant correlation between [^{18}F]FDG uptake and the measured enzymatic activities of either HK or G6Pase, in support of the realization that [^{18}F]FDG uptake and metabolism are complex mechanisms with no single step in control of [^{18}F]FDG uptake. We found a significant inverse correlation between measured HK and G6Pase activities. Furthermore, the positive correlation of SUVmax with the regression intercepts of the inverse correlations (maximal enzymatic activities) suggests that both enzymes play a role in the accumulation of FDG6P. The results identify two ovarian cancer phenotypes, one with elevated HK activity and low G6Pase activity, and another with the opposite characteristics. Future research must address larger patient populations or relevant pre-clinical models that further explore the fundamental mechanisms.

Compliance with Ethical Standards

Conflict of Interest

The authors declare that they have no conflict of interest.

Ethics Approval

All procedures performed in studies involving human participants were in accordance with the ethical standards of the institutional and/or national research committee and with the 1964 Helsinki Declaration and its later amendments or comparable ethical standards.

Informed Consent

Twenty-three patients were enrolled prospectively after both oral and written information and signed consent. Six patients were enrolled retrospectively, with previously obtained formal consent to retroactive use of tissue still valid.

References

1. Siegel R, Ma J, Zou Z, Jemal A (2014) Cancer statistic 2014. CA Cancer J Clin 64:9–29
2. Risum S, Høgdall C, Loft A, Berthelsen AK, Høgdall E, Nedergaard L, Lundvall L, Engelholm SA (2010) Does the use of diagnostic PET/CT cause stage migration in patients with primary advanced ovarian cancer? Gynecol Oncol 116:395–398
3. Musto A, Rampin L, Nanni C, Marzola MC, Fanti S, Rubello D (2011) Present and future of PET and PET/CT in gynaecologic malignancies. Eur J Radiol 78:12–20
4. Nakamura K, Hongo A, Kodama J, Hiramatsu Y (2012) The pretreatment of maximum standardized uptake values (SUVmax) of the primary tumor is predictor for poor prognosis for patients with epithelial ovarian cancer. Acta Med Okayama 66:53–60
5. Schwartz L, Supuran CT, Alfarouk KO (2017) The Warburg effect and the hallmarks of cancer. Anti Cancer Agents Med Chem 17:164–170
6. Macheda ML, Rogers S, Best JD (2005) Molecular and cellular regulation of glucose transporter (GLUT) proteins in cancer. J Cell Physiol 202:654–662
7. Shinohara Y, Yamamoto K, Kogure K, Ichihara J, Terada H (1994) Steady state transcript levels of the type II hexokinase and type 1 glucose transporter in human tumor cell lines. Cancer Lett 82:27–32
8. Kurokawa T, Yoshida Y, Kawahara K, Tsuchida T, Okazawa H, Fujibayashi Y, Yonekura Y, Kotsuji F (2004) Expression of GLUT-1 glucose transfer, cellular proliferation activity and grade of tumor correlate with [F-18]-fluorodeoxyglucose uptake by positron emission tomography in epithelial tumors of the ovary. Int J Cancer 109:926–932
9. Yen TC, See LC, Lai CH, Yah-Huei CW, Ng KK, Ma SY, Lin WJ, Chen JT, Chen WJ, Lai CR, Hsueh S (2004) ^{18}F-FDG uptake in squamous cell carcinoma of the cervix is correlated with glucose transporter 1 expression. J Nucl Med 45:22–29

10. Nagamatsu A, Umesaki N, Li L, Tanaka T (2010) Use of ^{18}F-fluorodeoxyglucose positron emission tomography for diagnosis of uterine sarcomas. Oncol Rep 23:1069–1076
11. Nakamura K, Kodama J, Okumura Y, Hongo A, Kanazawa S, Hiramatsu Y (2010) The SUVmax of ^{18}F-FDG PET correlates with histological grade in endometrial cancer. Int J Gynecol Cancer 20:110–115
12. Tsujikawa T, Yoshida Y, Kiyono Y, Kurokawa T, Kudo T, Fujibayashi Y, Kotsuji F, Okazawa H (2011) Functional oestrogen receptor α imaging in endometrial carcinoma using 16α-[^{18}F]fluoro-17β-oestradiol PET. Eur J Nucl Med Mol Imaging 38:37–45
13. Tong SY, Lee JM, Ki KD, Choi YJ, Seol HJ, Lee SK, Huh CY, Kim GY, Lim SJ (2012) Correlation between FDG uptake by PET/CT and the expressions of glucose transporter type 1 and hexokinase II in cervical cancer. Int J Gynecol Cancer 22:654–658
14. Park SI, Suh DS, Kim SJ, Choi KU, Yoon MS (2013) Correlation between biological marker expression and F-fluorodeoxyglucose uptake in cervical cancer measured by positron emission tomography. Onkologie 36:169–174
15. Zhao Z, Yoshida Y, Kurokawa T, Kiyono Y, Mori T, Okazawa H (2013) ^{18}F-FES and ^{18}F-FDG PET for differential diagnosis and quantitative evaluation of mesenchymal uterine tumors: correlation with immunohistochemical analysis. J Nucl Med 54:499–506
16. Jo MS, Choi OH, Suh DS, Yun MS, Kim SJ, Kim GH, Jeon HN (2014) Correlation between expression of biological markers and [^{18}F]fluorodeoxyglucose uptake in endometrial cancer. Oncol Res Treat 37:30–34
17. Marcolongo P, Fulceri R, Gamberucci A et al (2012) Multiple roles of glucose-6-phosphatases in pathophysiology: state of the art and future trends. Biochim Biophys Acta 1830:2608–2618
18. Robey RB, Hay N (2006) Mitochondrial hexokinases, novel mediators of the antiapoptotic effects of growth factors and Akt. Oncogene 25:4683–4696
19. Van Schaftingen E, Gerin I (2002) The glucose-6-phosphatase system. Biochem J 362:513–532
20. Boellaard R, Delgado-Bolton R, Oyen WJ, Giammarile F, Tatsch K, Eschner W, Verzijlbergen FJ, Barrington SF, Pike LC, Weber WA, Stroobants S, Delbeke D, Donohoe KJ, Holbrook S, Graham MM, Testanera G, Hoekstra OS, Zijlstra J, Visser E, Hoekstra CJ, Pruim J, Willemsen A, Arends B, Kotzerke J, Bockisch A, Beyer T, Chiti A, Krause BJ, European Association of Nuclear Medicine (EANM) (2015) FDG PET/CT: EANM procedure guidelines for tumour imaging: version 2.0. Eur J Nucl Med Mol Imaging 42:328–354
21. Bradford MM (1976) A rapid and sensitive method for the quantitation of microgram quantities of protein utilizing the principle of protein-dye binding. Anal Biochem 72:248–254
22. Taussky HH, Shorr E (1953) A microcolorimetric method for the determination of inorganic phosphorus. J Biol Chem 202:675–685
23. Yamamoto Y, Oguri H, Yamada R, Maeda N, Kohsaki S, Fukaya T (2008) Preoperative evaluation of pelvic masses with combined ^{18}F-fluorodeoxyglucose positron emission tomography and computed tomography. Int J Gynaecol Obstet 102:124–127
24. Kitajima K, Suzuki K, Senda M, Kita M, Nakamoto Y, Onishi Y, Maeda T, Yoshikawa T, Ohno Y, Sugimura K (2011) FDG-PET/CT for diagnosis of primary ovarian cancer. Nucl Med Commun 32:549–553
25. Tanizaki Y, Kobayashi A, Shiro M, Ota N, Takano R, Mabuchi Y, Yagi S, Minami S, Terada M, Ino K (2014) Diagnostic value of preoperative SUVmax on FDG-PET/CT for the detection of ovarian cancer. Int J Gynecol Cancer 24:454–460
26. Jin Z, Gu J, Xin X, Li Y, Wang H (2014) Expression of hexokinase 2 in epithelial ovarian tumors and its clinical significance in serous ovarian cancer. Eur J Gynaecol Oncol 35:519–524
27. Pedersen P, Mathupala S, Rempel A et al (2002) Mitochondrial bound type II hexokinase: a key player in the growth and survival of many cancers and an ideal prospect for therapeutic intervention. Biochim Biophys Acta 1555:14–20
28. Gejl M, Egefjord L, Lerche S, Vang K, Bibby BM, Holst JJ, Mengel A, Møller N, Rungby J, Brock B, Gjedde A (2012) Glucagon-like peptide-1 decreases intracerebral glucose content by activating hexokinase and changing glucose clearance during hyperglycemia. J Cereb Blood Flow Metab 32:2146–2152
29. Gejl M, Lerche S, Egefjord L et al (2013) Glucagon-like peptide-1 (GLP-1) raises blood-brain glucose transfer capacity and hexokinase activity in human brain. Front Neuroenerg 5:2
30. Abbadi S, Rodarte JJ, Abutaleb A, Lavell E, Smith CL, Ruff W, Schiller J, Olivi A, Levchenko A, Guerrero-Cazares H, Quinones-Hinojosa A (2014) Glucose-6-phosphatase is a key metabolic regulator of glioblastoma invasion. Mol Cancer Res 12:1547–1559
31. Guo T, Chen T, Gu C, Li B, Xu C (2015) Genetic and molecular analyses reveal G6PC as a key element connecting glucose metabolism and cell cycle control in ovarian cancer. Tumour Biol 36:7649–7658
32. Hart WR (2005) Borderline epithelial tumors of the ovary. Mod Pathol 18:S33–S50
33. Patra KC, Wang Q, Bhaskar PT, Miller L, Wang Z, Wheaton W, Chandel N, Laakso M, Muller WJ, Allen EL, Jha AK, Smolen GA, Clasquin MF, Robey RB, Hay N (2013) Hexokinase 2 is required for tumor initiation and maintenance and its systemic deletion is therapeutic in mouse models of cancer. Cancer Cell 24:213–228